CHAPTER 4

Design and testing of tunable isolator

4.1 Introduction

The previous chapter discussed the development of a practical variable stiffness spring for implementation on a LIVE isolator. It is also necessary to implement a variable damping mechanism in the isolator. The isolator will be designed to demonstrate that it is possible to build a tunable vibration isolator and will therefore not be designed for a specific application.

The isolator will be tested on a servo-hydraulic actuator in the laboratory and the capabilities of the actuator must be kept in mind in the design phase of the isolator.

4.2 Variable damping mechanism

As described previously, one of the aims is to be able to change the damping of the isolator. Structural damping as well as viscous damping is present in the isolator. In order to change the damping of the isolator, one or both of these damping constants must be increased. To change the structural damping of the spring or rolling membranes is quite difficult and therefore the viscous damping will be changed.

The main source of the viscous damping is the fluid going through the port at high velocity. This causes flow losses that in turn are reflected as viscous damping. The flow losses are created when a velocity difference exists between the fluid and surrounding bodies like at the port surface. These flow losses are further increased when turbulent flow or separation occurs at sharp edges, corners or holes. Therefore it will be possible to increase the flow losses by either increasing the surface contact area between the high-speed fluid in the port and the surrounding port or by inducing turbulent flow and flow separation in the port. To increase the surface contact area is not an easily executable option, so the second option was chosen.

The mechanism used must satisfy the following criteria:

- The mechanism must be easily operatable from outside the port.
- The connections to the outside must be watertight.
- It is preferable that the mechanism does not change the volume inside the isolator due to the problems it will create.
- In order to obtain maximum damping change, the minimum damping of the mechanism must be as low as possible.

There are basically two options to choose from, translational and rotational movement. With translational movement a plate or pen would be pushed further and further into the port to increase flow losses. The rotational concept would have a plate mounted in the port. When the plate is orientated vertically, there will be very little flow losses. As the angle of the plate increases, the flow losses will increase due to the turbulent flow over the edges of the plate. Maximum damping will occur when the plate is horizontal.

The translational movement will have a problem with either sealing or changing the volume. Compared to that, the rotational movement will have no influence on the volume and by connecting the ends of the plate to shafts will make the sealing very easy with normal oil seals. Therefore the rotational concept was chosen and the plate that would be inserted into the port is depicted in Figure 4. 1.

The thin plate like part fits into the port. The plate is thinner than the diameter of the port so that the flow will not be shut off completely, but only partly restricted. The cylindrical parts are for sealing and holding it in place. The ends are outside the port and the shaft can therefore be turned from the outside by some sort of actuator or motor.

Because rotation is used, an electrical motor would be the simple answer for turning the shaft. The only problem with a DC motor is position control. The angular position of the motor is very important and therefore some sort of position feedback will be needed if a DC motor is used. Another type of electrical motor that can be used is a stepper motor. Stepper motors are electrical motors that are controlled step by step and are therefore position control motors. They are used extensively in things

like printers and plotters where position control is needed. They are very cheap in comparison with a DC motor with shaft encoder. There is also no need for a closed loop control system to do position control on the motor.

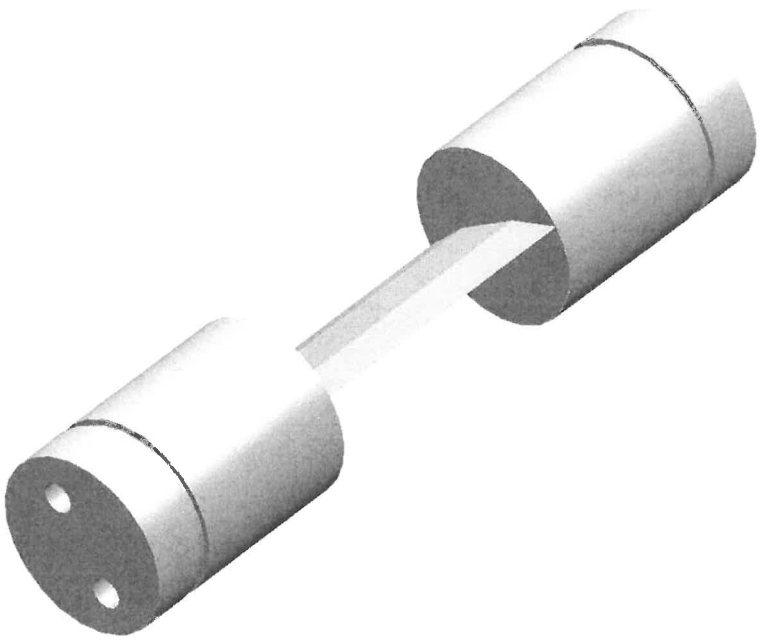

Figure 4. 1 Plate to be inserted in port

Although these types of motors are well known, the working principle of the motors and the control of them are not well known and therefore it is addressed in detail in Appendix C.

The circuitry developed to drive the stepper motor is depicted in Figure 4. 2.

4.3 Design of adaptable isolator

In this section the parameters of the isolator will be determined. The stiffness has already been determined to be variable between 80 000 N/m and 200 000 N/m. The loss factor of the structural damping has also been determined as being around 0.1. These values will now be used to determine the other parameters like port length, diameter and area ratio.

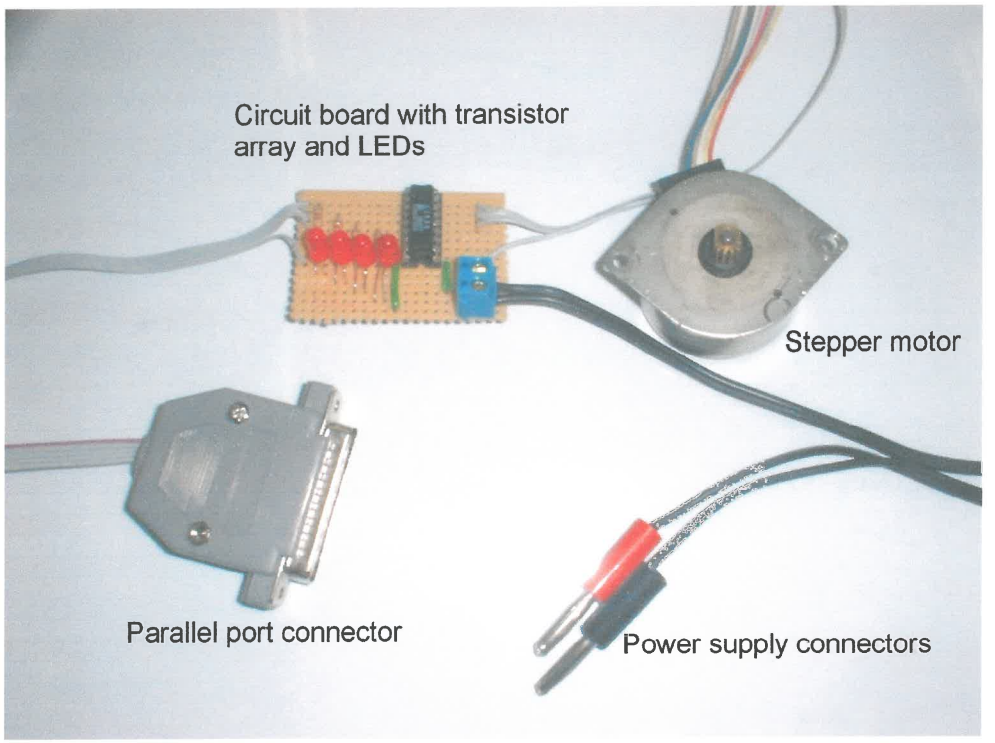

Figure 4. 2 Stepper motor circuitry

Before the design can be done, a few decisions have to be made regarding the properties of the isolator. The isolation frequency, mass and port length have to be chosen. The following values have been chosen:

Table 4. 1 Chosen parameters for isolator

Property	**Value**
Isolation frequency	30 Hz
Mass	4 kg
Port length	100 mm

The servo-hydraulic actuator can easily give excitation up to 50 Hz and therefore the 30 Hz isolation frequency was chosen. This will be the centre isolation frequency (for a stiffness of about 140 000 N/m). A mass of 4 kg was estimated to be a good representative value of what the mass of the isolator parts will be. It is not foreseen to add extra weights to the isolator to improve performance of the isolator. A port length

of 100 mm is sufficient to put the damping mechanism in without being limited by space.

There is another consideration regarding the stiffness. In the LIVE isolator, it is necessary to seal the fluid inside, while still allowing the port to move relative to the reservoir. This is usually done by moulding rubber in-between the two parts that act as a seal but also as the spring for the system as shown in Figure 4. 3.

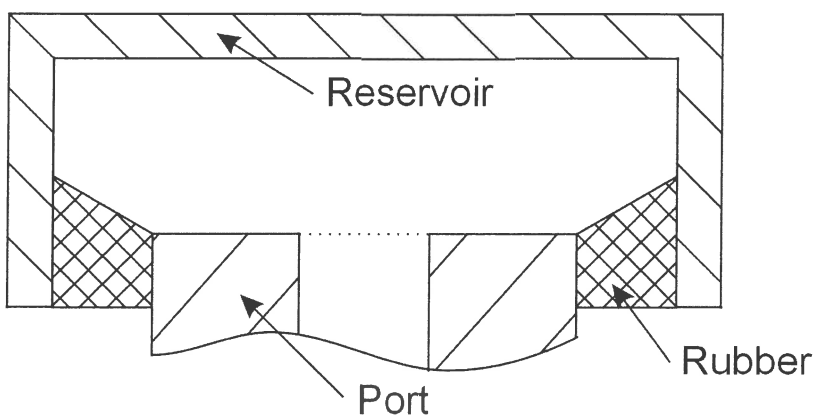

Figure 4. 3 Moulded rubber seal

In this case it is not preferable at all to add more stiffness to the system because it will decrease the overall stiffness change that can be achieved. Therefore another option must be considered.

Rolling diaphragms are sealing devices available on the market that seal two circular bodies while allowing movement with almost no stiffness. The diaphragms work as shown in Figure 4. 4.

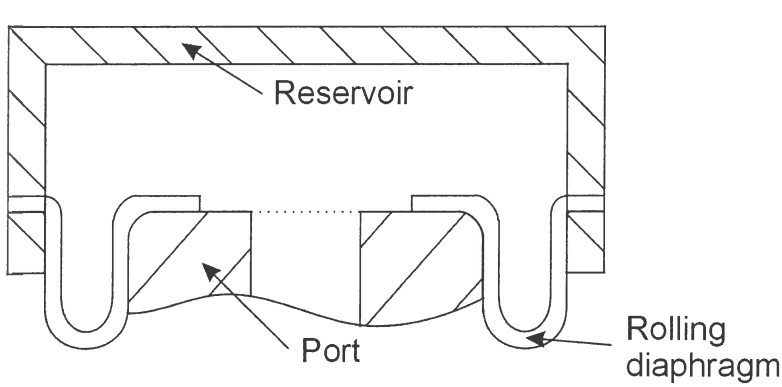

Figure 4. 4 Rolling diaphragm seal

These diaphragms are made of Nitrial rubber impregnated with a cotton woven sheet to prevent stretching. One other very important aspect of the diaphragms for the application is that they do not have a centre position and can work in any position. It will be remembered that the variable stiffness spring centre position changes as the leafs are separated. With a moulded rubber seal this would cause a major problem, but using rolling diaphragms solves it.

These diaphragms are therefore ideal for this application and will be used instead of moulded rubber. One problem with the diaphragms is availability. They can only be obtained in 3 sizes of which 2 are very small. Therefore the diaphragm determines the outside diameter of the reservoir. The diaphragm used is a Simrit Long-stroke-rolling diaphragm, type BFA 80x70x30. Figure 4. 5 gives the installation details for these diaphragms.

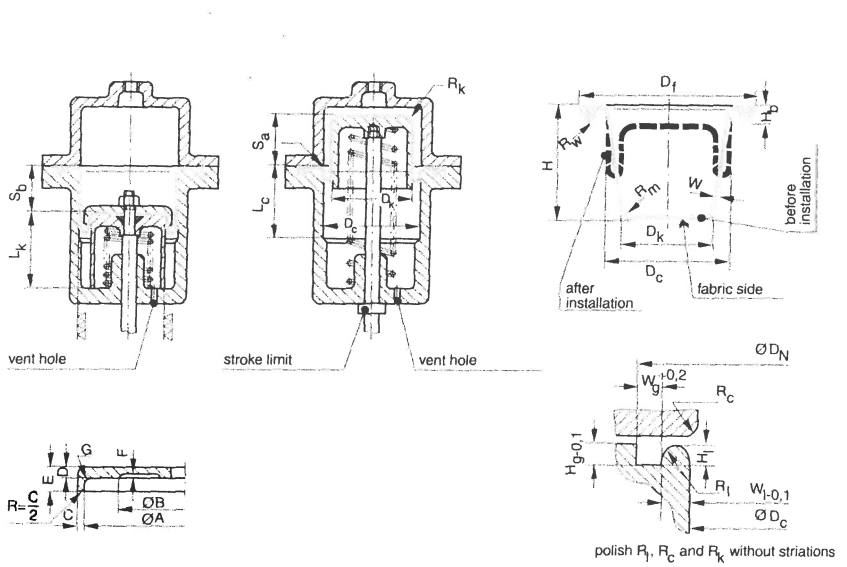

Figure 4. 5 Installation details for rolling diaphragms (Simrit)

Therefore the diameters of the reservoir will be as shown in Figure 4. 6.

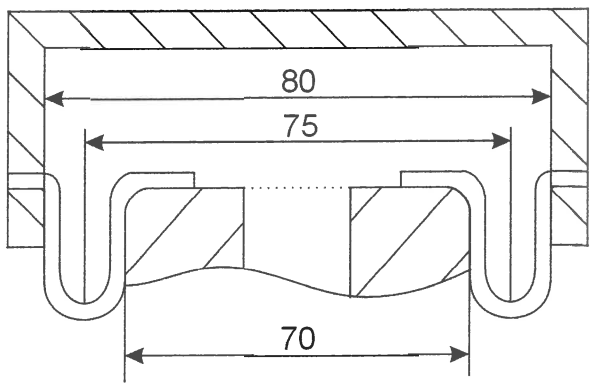

Figure 4. 6 Dimensions of reservoir

For calculation purposes, the outside diameter of the reservoir is the diameter of the piston that is moving upwards. Due to the fact that the diaphragm is also moving upwards, the outside diameter can be taken as 75 mm.

With all the values determined and chosen, the last parameter, the port diameter, can be calculated. The equation for the undamped isolation frequency will be used for this purpose due to simplicity. The equation is the following:

$$\omega_a = \sqrt{\frac{-k}{m_B\left(1-\frac{A_b}{A_a}\right)\frac{A_b}{A_a}}} \tag{4.1}$$

with

$$m_B = \rho \ell A_a \tag{4.2}$$

The area of the port and therefore the diameter of the port can be calculated as 25.5 mm. This will be rounded off to 25 mm. It is important to notice that the design is not done 100% accurately due to the fact that it is not necessary to have the isolation frequency at exactly 30 Hz. If it is 20% lower or higher, it will not matter because it is not designed for a specific application.

If such an isolator is designed for a specific application however, the design would be done in much more detail and greater care would be taken to accurately determine the masses, effective port length and the effect of damping. The damped isolation frequency would be used instead of the undamped isolation frequency and the flow

would be modelled to determine flow losses in the port. This would insure that the desired isolation frequency is obtained.

Figure 4. 7 show the transmissibility curves for the different stiffness values.

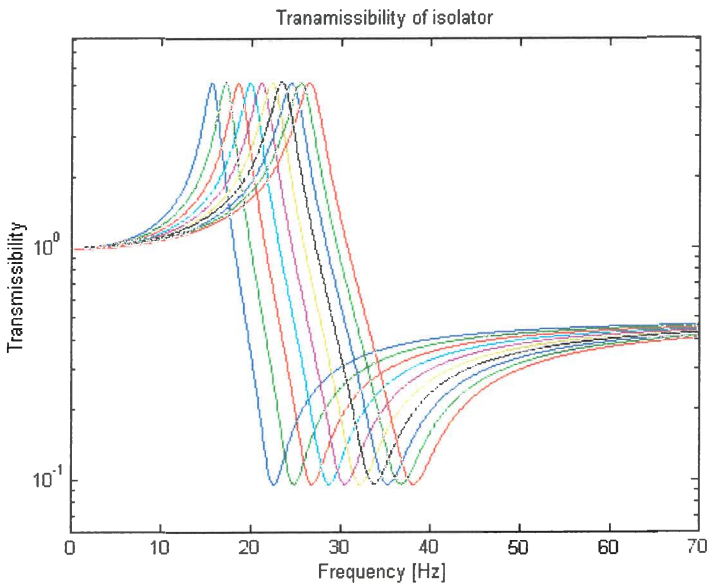

Figure 4. 7 Transmissibility form different stiffness values

This is what the designed isolator is supposed to be able to obtain, but this will probably change due to minor differences in the isolator itself. One factor that will certainly have an influence is the viscous damping value. It was taken as 0 for the above graphs, but will certainly not be 0 in the actual isolator.

Figure 4. 8 show a cross section through the designed isolator assembly.

It can be seen that edges around the port has been smoothed and rounded to minimise damping and that the rest of the design is quite simple and compact. It will be noted that there are no hole to fill the inside with water. The reason for this is that it was learnt from experience that it is almost impossible to get all the air out if the filling is done through a hole. Therefore the whole isolator was assembled while submerged in water to be sure that all the air is out of the reservoirs.

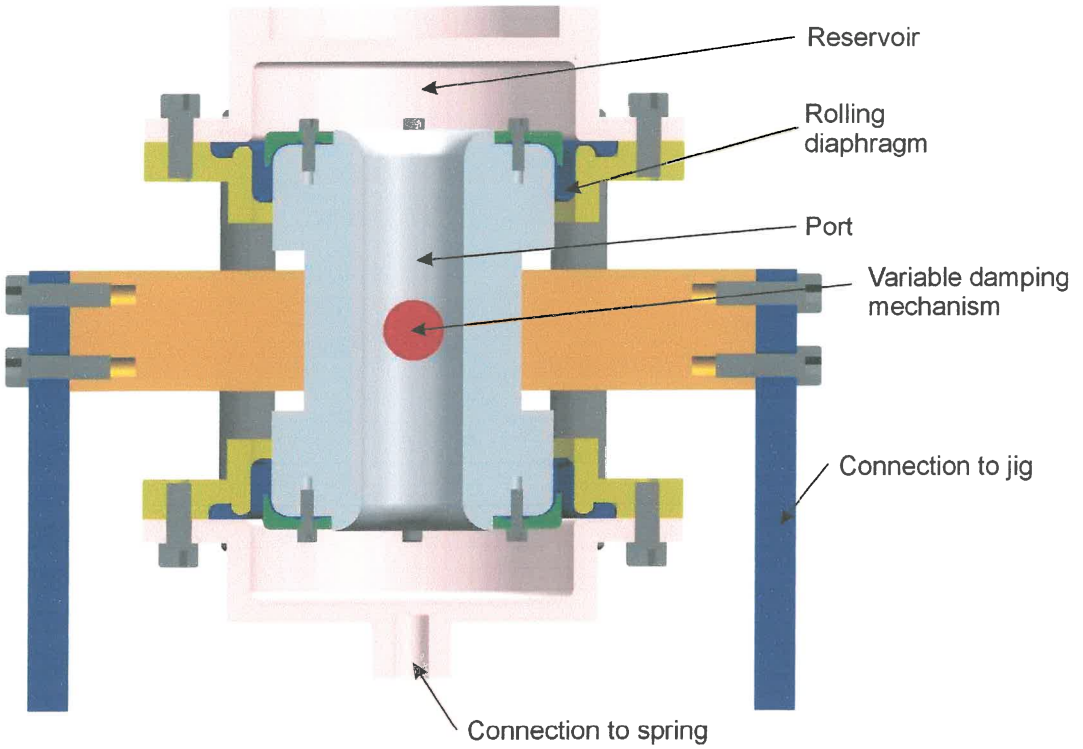

Figure 4. 8 Design of isolator

The isolator was manufactured, assembled and fitted to the variable stiffness spring to be tested. The whole assembly is depicted in Figure 4. 9.

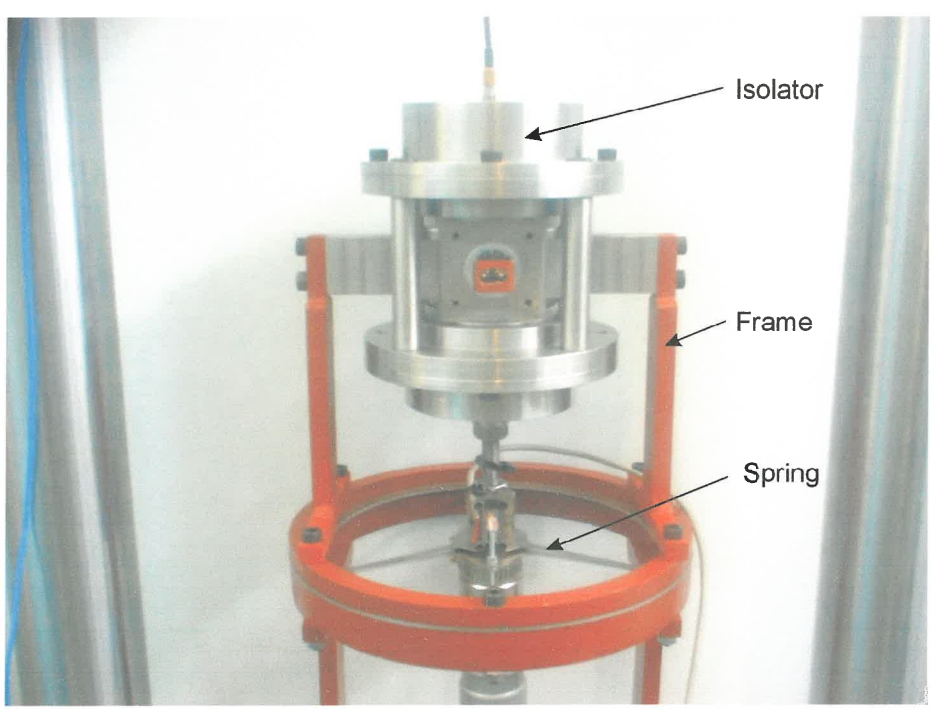

Figure 4. 9 Experimental setup

4.4 Testing of the isolator

As mentioned before, the isolator was tested on a servo-hydraulic actuator in the laboratory. To be able to measure transmissibility over the whole frequency range, the isolator has to be excited over the whole frequency range. This is usually done with one of the following two types of excitation:

- Random excitation
- Chirp excitation

Random excitation simply uses a white noise signal, usually band limited, to excite the structure. With chirp excitation, a sine wave is used of which the frequency is continuously swept from low to high frequencies to be able to excite all the frequencies. The two signals are represented graphically in Figure 4. 10.

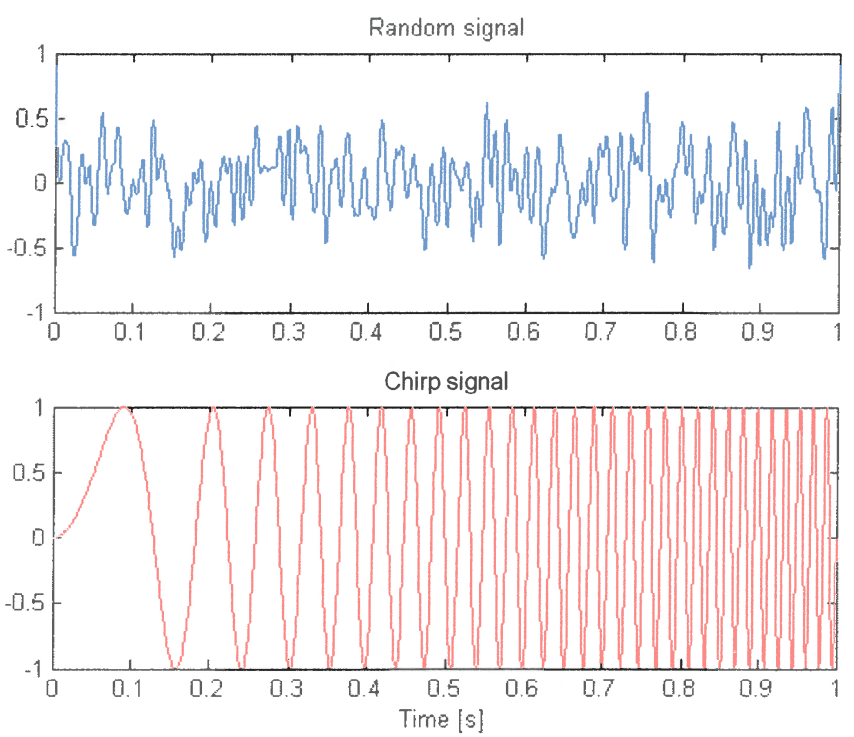

Figure 4. 10 Random and chirp excitation

The performance of the two excitation methods is application dependant and both were tested. It was found that random excitation worked better for the transmissibility measurement of the isolator. To measure the transmissibility, the acceleration of the input and output has to be measured and compared to each other. This was done by connecting an accelerometer to the actuator input and to the top of the isolator. Small 10 mV/g PCB ICP accelerometers were used together with signal conditioning amplifiers. The experimental setup is depicted in Figure 4. 11.

A Siglab measurement system was used to measure the signals and the transmissibility was calculated. The transmissibility is the H1 estimate between the two signals. Averaging is also used to smooth out the measured graphs and a Hanning window was used.

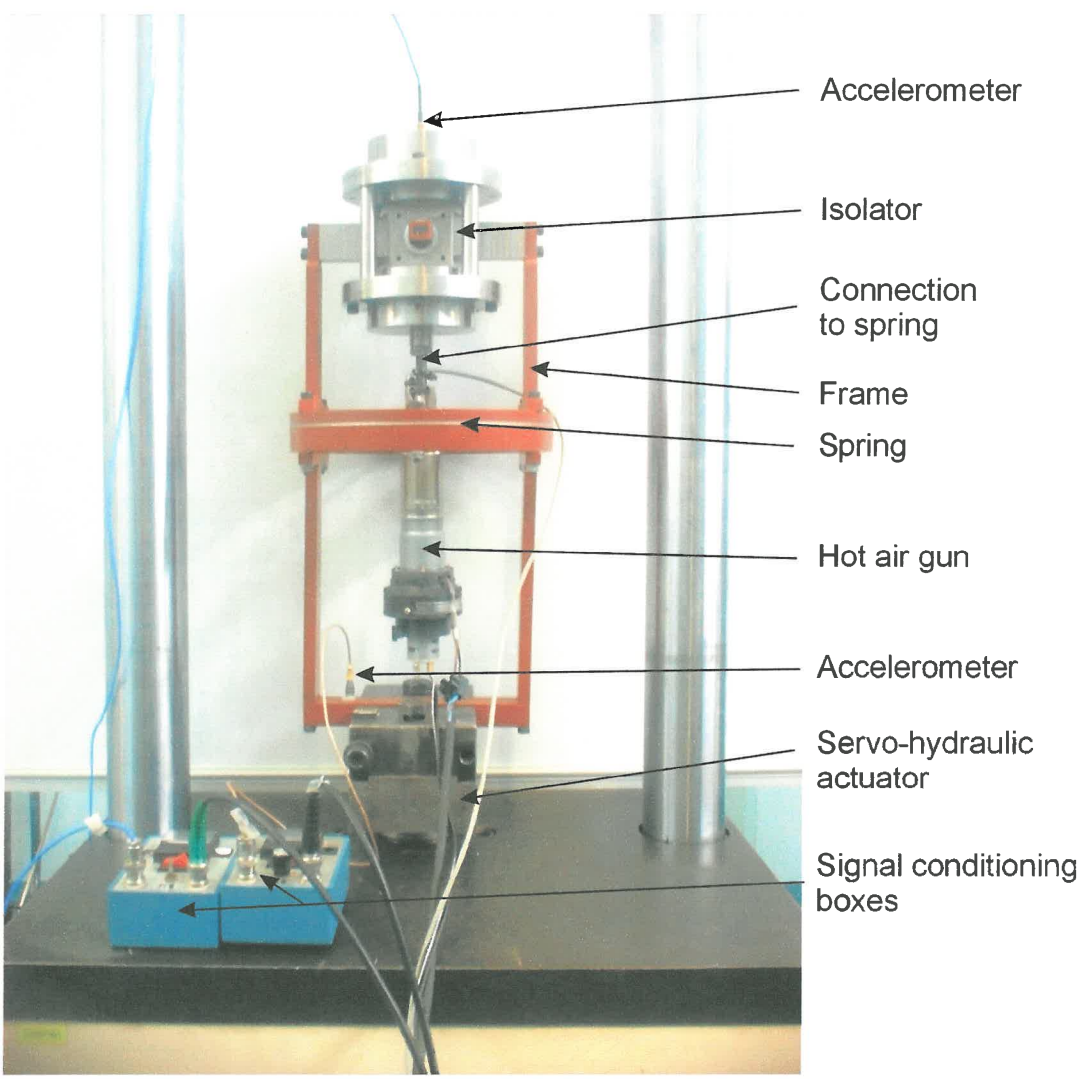

Figure 4. 11 Experimental setup

The first test was to measure the transmissibility of the isolator without any water inside. It is then essentially a mass-spring-damper system and the characteristics of the spring can be determined when connected to the isolator. The measured transmissibility is shown in Figure 4. 12.

It can very clearly be seen how the natural frequency of the system increases as the stiffness increases. The volt values in the legend refer to the setting on the spring controller (1 V = 2.3115 mm). It can also be seen that there is no isolation point present due to the absence of the water inside the isolator.

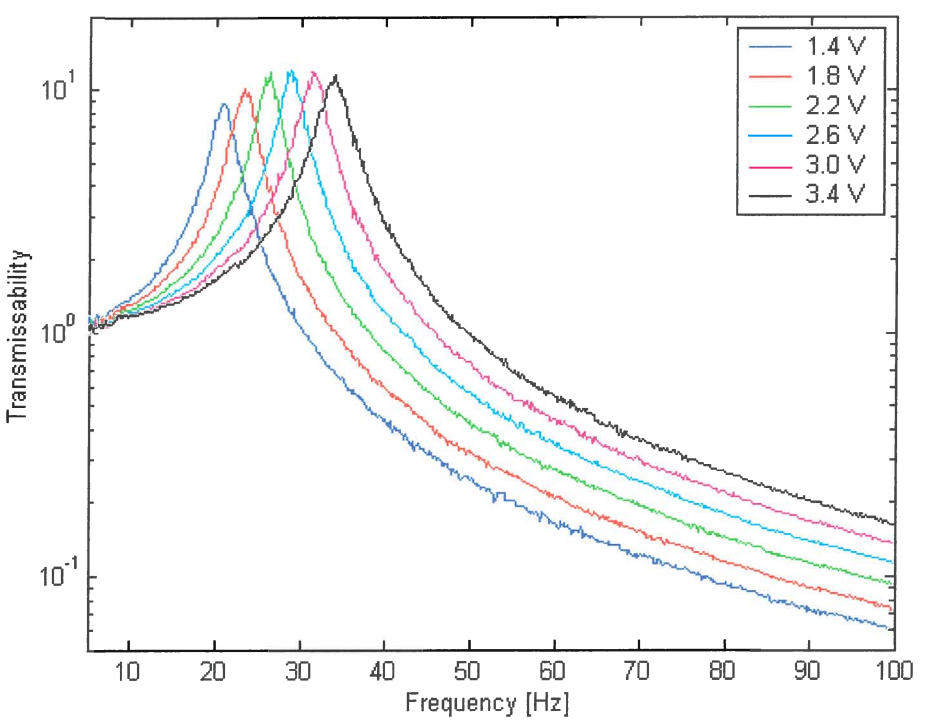

Figure 4. 12 Transmissibility of isolator without water

To determine the parameters of the spring from these graphs, a curve fit must be done on the graphs. The following equation gives the amplitude response of a mass-spring system with structural damping as given in equation (1.7):

$$|T| = \left| \frac{1 + i\eta}{1 - \left(\frac{\omega}{\omega_n}\right)^2 + i\eta} \right| \tag{4.3}$$

The Matlab function "nlinfit" was used to fit this equation to the measured graphs. It was of course possible to determine the mass of the system by measuring all the components. This was done and the total mass of the parts suspended by the spring weighed 4.287 kg. This was therefore used and the stiffness and loss factor were determined by fitting the graphs. Figure 4. 13 show the fit for the 1.4 V measurements.

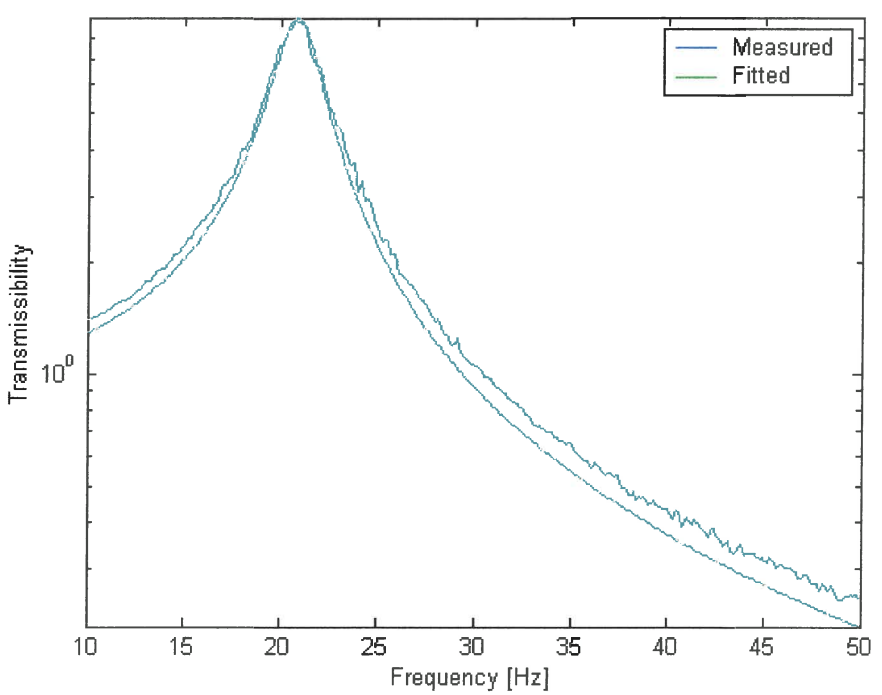

Figure 4. 13 Fitted transmissibility

It can be seen that the fit is quite accurate. By fitting all the graphs, the following results were obtained:

Table 4. 2 Fitted stiffness and damping values

Voltage	**1.4**	**1.8**	**2.2**	**2.6**	**3.0**	**3.4**
Stiffness [N/m]	73 328	92 098	115 690	140 530	167 040	193 930
Loss Factor	0.111	0.096	0.086	0.083	0.084	0.089

Figure 4. 14 give a comparison of the fitted stiffness values to the values obtained when testing the spring alone. It can be seen that the result are very similar and it looks as if the curve fit method used last produced better results at low separations. The structural damping loss factor is in the region of 0.09 for all the settings, so an average constant value of 0.0916 will be used in the following tests.

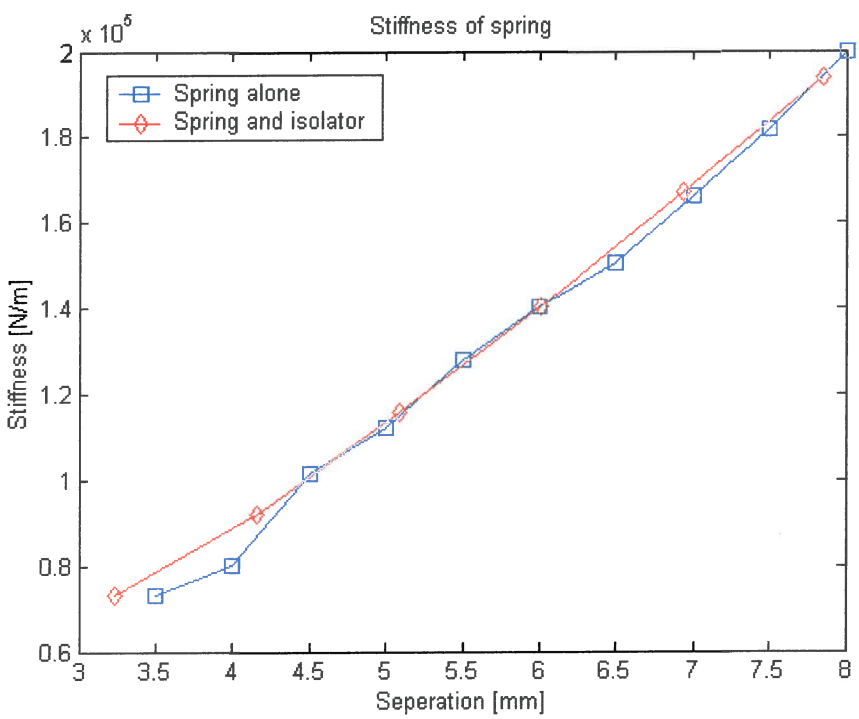

Figure 4. 14 Comparison of stiffness measurements

With the stiffness and damping of the spring determined, water was added to the isolator, the tests repeated and the transmissibility curves measured. The results are given in Figure 4. 15.

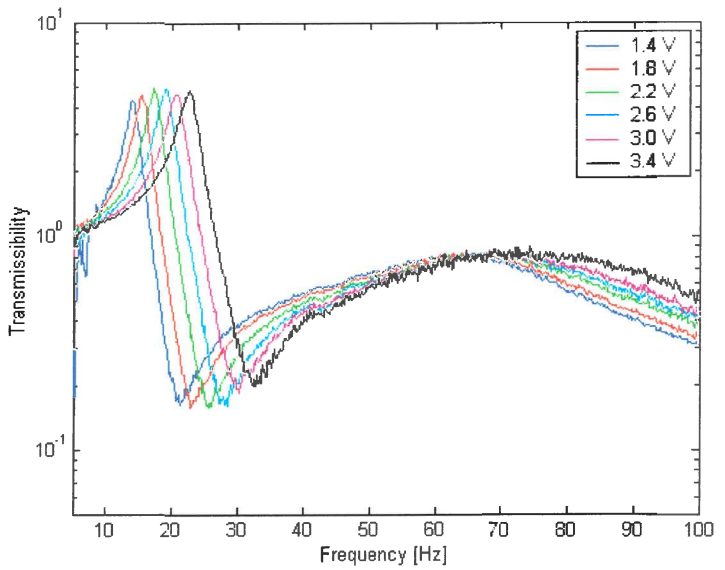

Figure 4. 15 Transmissibility with uncompressed water

The main observation from these graphs compared to the previous ones are the presence of the isolation point. The graphs still shift as the stiffness increases and it can be seen that the isolation frequency is shifted from 21 Hz to 33 Hz. This is quite a significant shift when the percentage difference is considered. Further it can be seen that an isolation of about 0.2 is obtained which is also quite significant. If the overall form of these graphs is compared to the form of the theoretical graphs in Figure 4. 7, it can be seen that they look similar up to about 40 Hz, but that the measured graph has a bump at about 65 Hz that is not present in the theoretical graphs. This can be explained by the fact that the water inside the isolator was not pressurised. Although the rolling diaphragms are lined with cotton to prevent it from stretching, it will still be able to expand a small amount. The effect of this is a second degree of freedom in the system created by the water being able to move without the port moving relative to the reservoir. The rolling diaphragms acts as the spring and the water as the mass and forms a spring-mass system with a natural frequency at about 65 Hz as can be seen in the graphs.

This second degree of freedom will cause serious problems when theoretical curves are fitted to the graphs. If the modal superposition principle is considered, it will be seen that the isolation point of the graph will be influenced the most by the second degree of freedom and that it will have a negative influence on the amount of isolation

achieved. The natural frequency will not be influenced very much. To try and eliminate this effect as far as possible, the water inside the isolator was pressurised. The effect of this will be that the diaphragms will stretch. That will increase the stiffness of the second degree of freedom significantly and shift its natural frequency hopefully high enough to have a negligible effect on the lower frequencies. It will therefore not be possible to take that second degree of freedom away completely, but it can be moved away far enough to eliminate its effect on the low frequencies.

This second degree of freedom is always a problem when building a LIVE isolator, because any deformation of the flexible element or any air trapped inside the isolator will cause such a second degree of freedom. It must therefore be ensured that this second natural frequency is high enough to have minimal effect on the lower frequencies.

The water inside the isolator was pressurised by changing the assembly process. It was not possible to measure the pressure inside the isolator, so the tests were redone to see if it had an effect. The results are shown in Figure 4. 16.

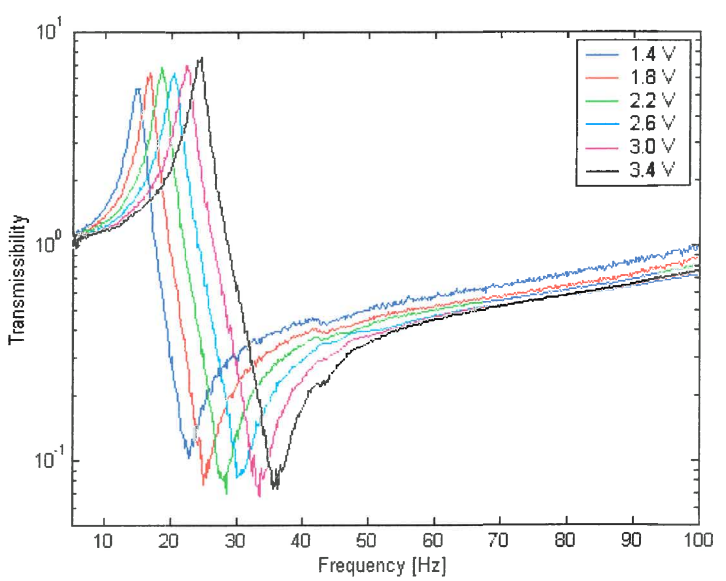

Figure 4. 16 Transmissibility with pressurised water

This time it can be seen that the bump is not present (or rather above 100 Hz). The amount of isolation has improved to about 0.1 and below. This can be seen as a good

amount of isolation. The fact the graphs still have a positive gradient at 100 Hz shows that the second natural frequency is still present but falls above 100 Hz. Therefore it can be assumed that the lower frequencies are not affected too much.

The numerical values of the measured natural and isolation frequencies are the following:

Table 4. 3 Measured natural and isolation frequencies

Voltage	**1.4**	**1.8**	**2.2**	**2.6**	**3.0**	**3.4**
Natural frequency [Hz]	14.625	16.75	18.5	20.375	22.25	24.5
Isolation frequency [Hz]	22.875	25	28.5	30.125	33.5	36.25

If the transmissibility curves for the different stiffness settings are combined to form one graph that shows the region of isolation that can be achieved, the graph in Figure 4. 17 is obtained.

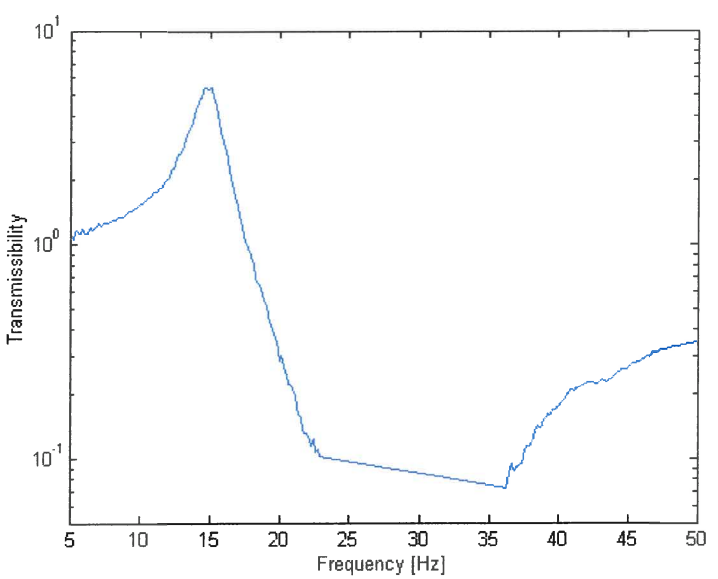

Figure 4. 17 Effective transmissibility of isolator

This gives an indication of what transmissibility the isolator can effectively obtain, although this cannot be obtained simultaneously. It must be mentioned that due to the

high pressure inside the isolator, the water did leak out slowly through the oil seals while in operation. This caused a problem and therefore some of the following tests like the optimisation test was done without the water being pressurised.

The next step is to fit theoretical graphs to these measured graphs to see whether they correlate. It may be suggested that all the parameters have already been obtained in the previous tests (without water) except possibly the viscous damping. This is true for the stiffness and structural damping, but with the addition of the water to the system, mass was added and would probably influence the mass of the isolator. Because it is not known exactly how the water flows inside the isolator, it is not possible to determine theoretically what the new mass of the isolator would be. It will off course be more than 4.287 kg, but could be more than the static mass of the system. Therefore the mass and viscous damping constant will be used as variables to fit theoretical graphs to the measured graphs. All other values will be kept constant as determined previously.

The equation that will be used for the theoretical graphs is the absolute non-dimensional transmissibility amplitude derived in equation (2.21). The equation is the following:

$$|T_r| = \left| \frac{k(1+i\eta) + i\omega c + \omega^2 m_b \left(1 - \frac{A_b}{A_a}\right)\frac{A_b}{A_a}}{k(1+i\eta) + i\omega c - \omega^2 \left[m + m_b \left(\frac{A_b}{A_a}\right)^2 \right]} \right| \tag{4.4}$$

with

$$\zeta = \frac{c}{2\left[m + m_b \left(\frac{A_b}{A_a}\right)^2 \right]\omega_n} \tag{4.5}$$

and

$$\omega_n = \sqrt{\frac{k}{m + m_b\left(\frac{A_b}{A_a}\right)^2}} \tag{4.6}$$

The fits were done with Matlab and results for the 1.8 V measurement are shown in Figure 4. 18. The complete set of results is presented in Appendix D.

It can be seen that the graphs fit very accurately below the isolation frequency, but that the second natural frequency has an influence above the isolation frequency due to the low amplitudes. The values fitted to the graphs are given in Table 4. 4.

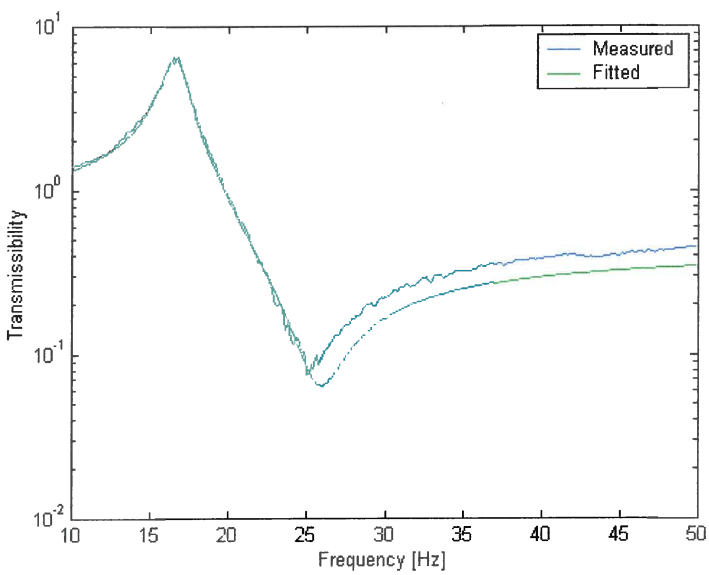

Figure 4. 18 Fitted transmissibility

Table 4. 4 Fitted values

Voltage	**1.4**	**1.8**	**2.2**	**2.6**	**3.0**	**3.4**
Mass [kg]	4.4239	4.4512	4.5271	4.6063	4.5194	4.3896
Viscous damping	0.006	0.00007	0	0.0007	0	0
Stiffness [N/m]	73 328	92 098	115 690	140 530	167 040	193 930
Loss factor	0.0916					

It can be seen that virtually no viscous damping was present and it can be taken as 0 for the lowest damping setting. This shows how effective the design of the isolator is with its round edges and large port. All these tests have been done with the damping mechanism set to its lowest damping setting. To measure the effect of the variable damping mechanism, the transmissibility was measured for each stiffness setting with the damping mechanism set to 0%, 50% and 100% of the angle. This correlates to the plate inside the port being set vertical, at 45 degrees and horizontally respectively.

Figure 4. 19 give the results that were obtained for the 1.4 V stiffness setting.

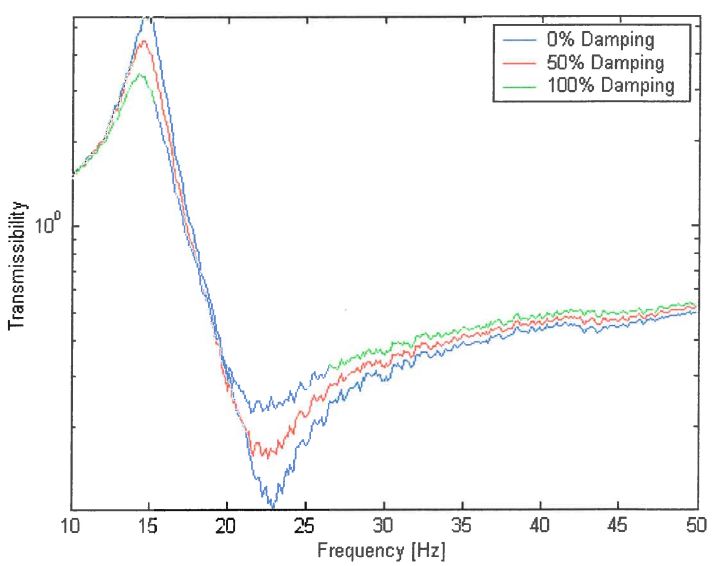

Figure 4. 19 Transmissibility for different damping settings

It can be seen that the variable damping mechanism works quite effectively and that the damping is increased significantly. Graphs were also fitted to the higher damping graphs, with the mass now kept constant at an average 4.486 kg. The only variable was therefore the viscous damping and the results are given in Figure 4. 20.

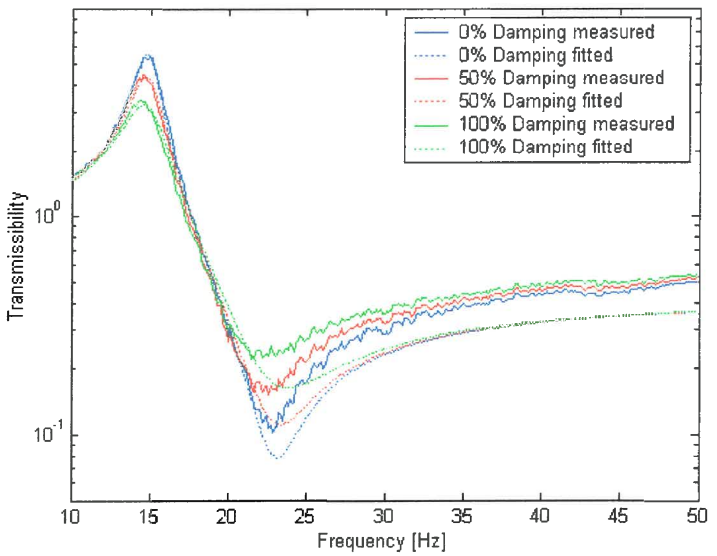

Figure 4. 20 Fitted transmissibility

The complete set of results is presented in Appendix D.

Again the fits are all very accurate below the isolation frequency, but not as good at and above the isolation frequency. The numerical values obtained for the viscous damping ratio are the following:

Table 4. 5 Fitted damping values

Volts	**1.4**	**1.8**	**2.2**	**2.6**	**3.0**	**3.4**
0% Damping	0.006	0.0001	0	0.0008	0	0
50% Damping	0.022	0.013	0.013	0.008	0.008	0.003
100% Damping	0.049	0.039	0.034	0.029	0.025	0.020

The slightly different 0% damping values is due to the constant mass of 4.486 kg that was used for these fits. It can be seen that the viscous damping constant values are quite low but that they increase as the damping is set higher. There is also a trend of a decreasing damping value as the stiffness is increased. This trend can be explained by means of the following equation:

$$\zeta = \frac{c}{2\sqrt{km}} \tag{4.7}$$

If the viscous damping coefficient, c, is taken as constant and the stiffness is increased, then the damping ratio, ζ, must decrease. The following average values for the viscous damping ratio can be determined:

Table 4. 6 Average damping values

0% Damping	0.001
50% Damping	0.011
100% Damping	0.033

The accuracy of these values can be debated due to their small values, but the values obtained show the tendency very clearly.

These tests showed that a successful tunable LIVE isolator has been designed and built. Its isolation frequency can be varied from 22.8 Hz to 36.2 Hz that is a 58.77 % shift in isolation frequency. The amount of isolation achieved at the isolation frequency was 0.078 on average. The damping of the isolator can also be changed with a viscous damping constant ranging from 0.001 to 0.033. The next section will deal with the design and implementation of a control system to automatically tune the isolator to perform optimally for specific excitation conditions.

4.5 Design and implementation of isolator control system

To be able to have a practical isolator, the isolator must be able to automatically tune itself and adapt to certain excitation conditions. The design and implementation of such a control system will be addressed in this section. The purpose is however not to design an optimal control system, but rather to prove that it is possible to implement such a control system and that it works in practice.

In principle the control system must be able to measure the performance of the isolator and must then vary the parameters (stiffness and damping) to obtain the best settings for the current excitation conditions. Thereafter the control system must keep the isolator at those settings and detect when the excitation conditions change and determine new settings. A block diagram of the global design of the control system is shown in Figure 4. 21.

It will be assumed that semi-stationary excitation conditions will be present meaning that the excitation conditions will be constant for a certain period of time to allow for the optimisation.

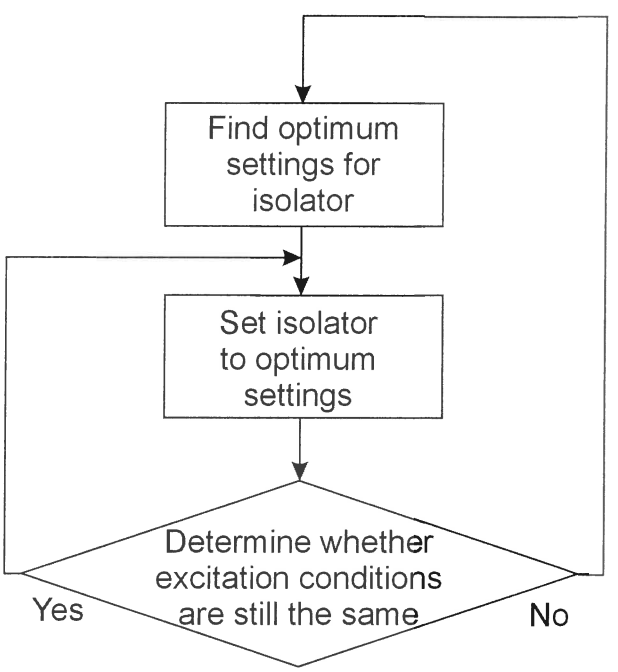

Figure 4. 21 Global design of control system

On implementation of the stepper motor on the variable damping mechanism, it was discovered that the torque needed to turn the shaft was more than what the motor could deliver due to the oil seals' friction. Therefore a gearbox would be needed to turn the shaft. Although possible, it was decided not to solve the problem due to the fact that the principle needed to be proven by the control system will be proven sufficiently by only changing the stiffness.

One parameter that has to be decided on is the criteria that will be used to evaluate the performance of the isolator. This must be a single value that can be used in the optimisation process to determine the performance of the system. Ideally this parameter must not be sensitive to changes in amplitude of excitation, but must be sensitive to frequency changes and changes in the ratio between noise levels and excitation levels. For the parameter to be insensitive to amplitude changes, the input and output signals must be measured and used to determine the parameter instead of only the output. The criterion that was chosen is the RMS ratio. This is calculated as follow:

$$RMS_{Ratio} = \frac{RMS_{Output}}{RMS_{Input}} \tag{4.8}$$

Therefore the time domain signals of the input and output will be measured and their RMS values determined. Then the RMS value of the output will be divided by the RMS value of the input to get the RMS ratio value.

The same experimental setup was used for this test as was used for the transmissibility measurements, except that the two accelerometers were not connected to the Siglab measurement system, but to the analog to digital converter that was used to control the wax actuator. The control system was implemented in Matlab and the optimisation algorithm "fminbnd" was used to determine the optimum stiffness setting for the current excitation. "Fminbnd" is a scalar bound non-linear function minimization. It uses the golden section method as well as parabolic interpolation to determine the minimum of a single variable continuous function.

An upper and lower bound can be supplied for the variable that would be the voltage setting in this case. The bounds were therefore set to 1.4 V and 3.4 V. In each loop of the function the stiffness was set to the desired value and then the time signals of the accelerometers were measured and the RMS ratio determined and sent back to the function. This is then repeated until the minimum RMS ratio has been reached according to certain tolerances. Figure 4. 22 give a graphical representation of the optimisation program.

Because an optimisation algorithm was used, the "guesses" of the stiffness values are actually calculated and not just random guesses. This part of the control system was programmed and tested on the servo-hydraulic actuator. The isolator was excited by different constant frequency sine waves and then the control system was activated and the response was recorded. The control system chose a random stiffness setting at the beginning to be able to get a value to start from and then started to search for the optimum position. Figure 4. 23 show how the RMS ratio improved as the number of iterations increased for the different excitation frequencies.

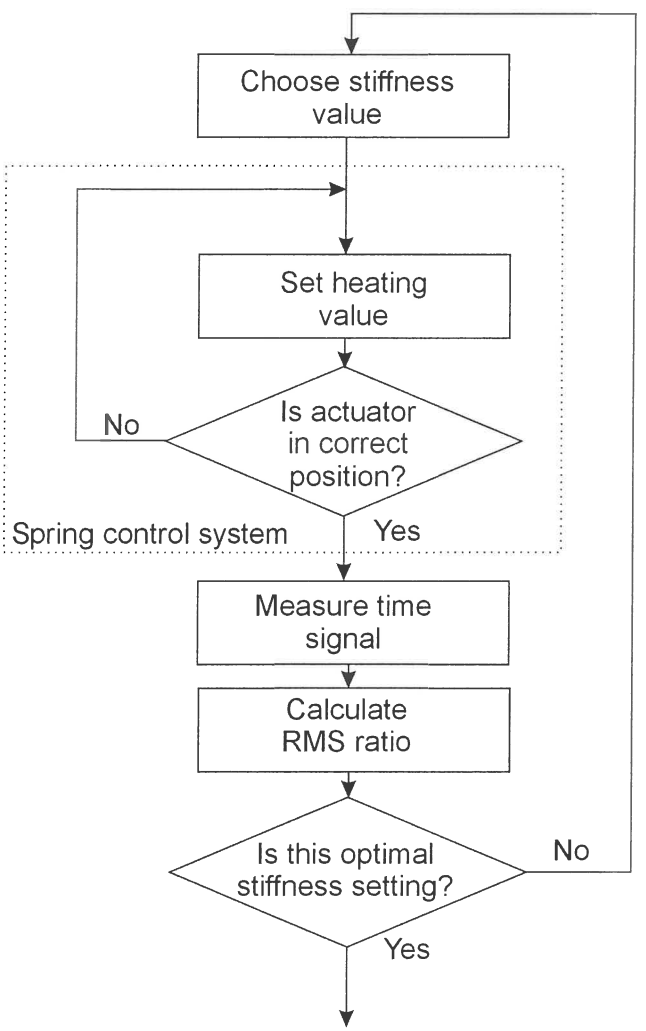

Figure 4. 22 Optimisation program

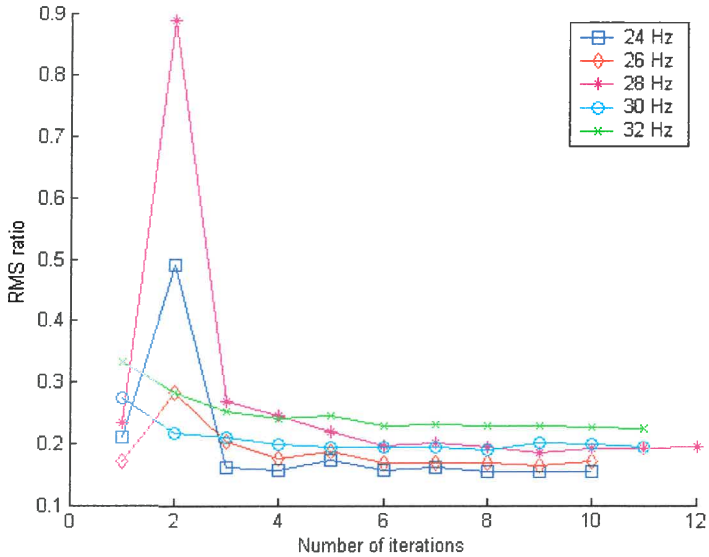

Figure 4. 23 Optimisation performance

Each time the optimal point was reached within 10 to 12 iterations. The RMS ratio values may seem a bit high, but it must be remembered that this is overall RMS values and not only at the isolation point. Although the servo-hydraulic actuator is supposed to excite the isolator only at a single constant frequency, other frequencies may also be excited. More significantly, these tests were done without pressurising the water inside the isolator, which decreased the amount of isolation achieved (see Figure 4. 15 and Figure 4. 16).

Numerical values obtained for spring settings and RMS ratio for the different excitation frequencies are the following:

Table 4. 7 Numerical values of optimum settings

Excitation frequency	Voltage setting for spring	RMS ratio
24 Hz	1.83 V	0.15
26 Hz	2.21 V	0.17
28 Hz	2.48 V	0.19
30 Hz	2.85 V	0.19
32 Hz	3.15 V	0.22

If the voltages that was obtained by the optimisation program are compared to the isolation frequency at different voltage settings as obtained from the transmissibility graphs (water not compressed), the graph in Figure 4. 24 is obtained. It can be seen that the results are similar and that it shows that the optimisation algorithm is working correctly and that the optimum setting was found every time.

A part of the control system that still needs to be addressed is the ability to keep the isolator at the determined settings until the excitation conditions change. This can be done by keeping the isolator at the determined settings and monitoring the RMS ratio of the isolator. If excitation conditions change, the RMS ratio will increase due to the fact that the isolator is not tuned to the excitation conditions any more. That is how the control system can sense when the excitation is changing and when the optimisation has to be started again. The whole control system is represented graphically in Figure 4. 25.

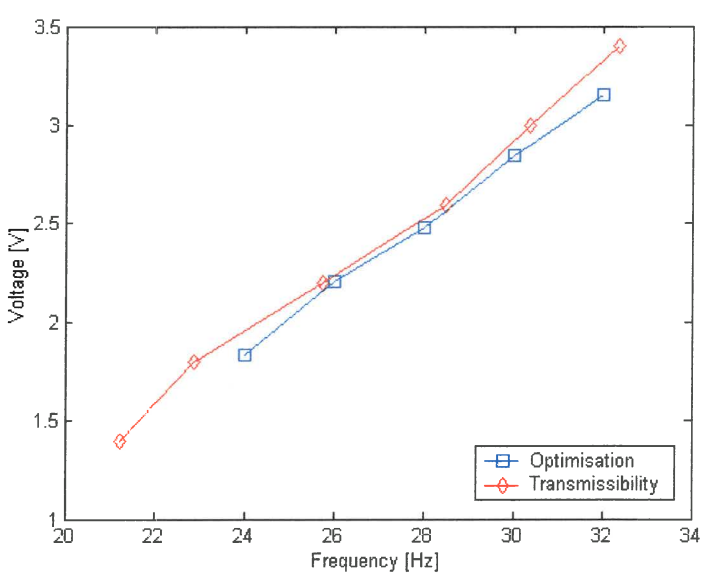

Figure 4. 24 Comparison of isolation frequencies

This control system will therefore keep the isolator at its best settings for the excitation conditions continuously. It is therefore proven that it is possible to implement a control system that can automatically change the settings of the isolator to be optimally tuned continuously. For the control system to change the damping as

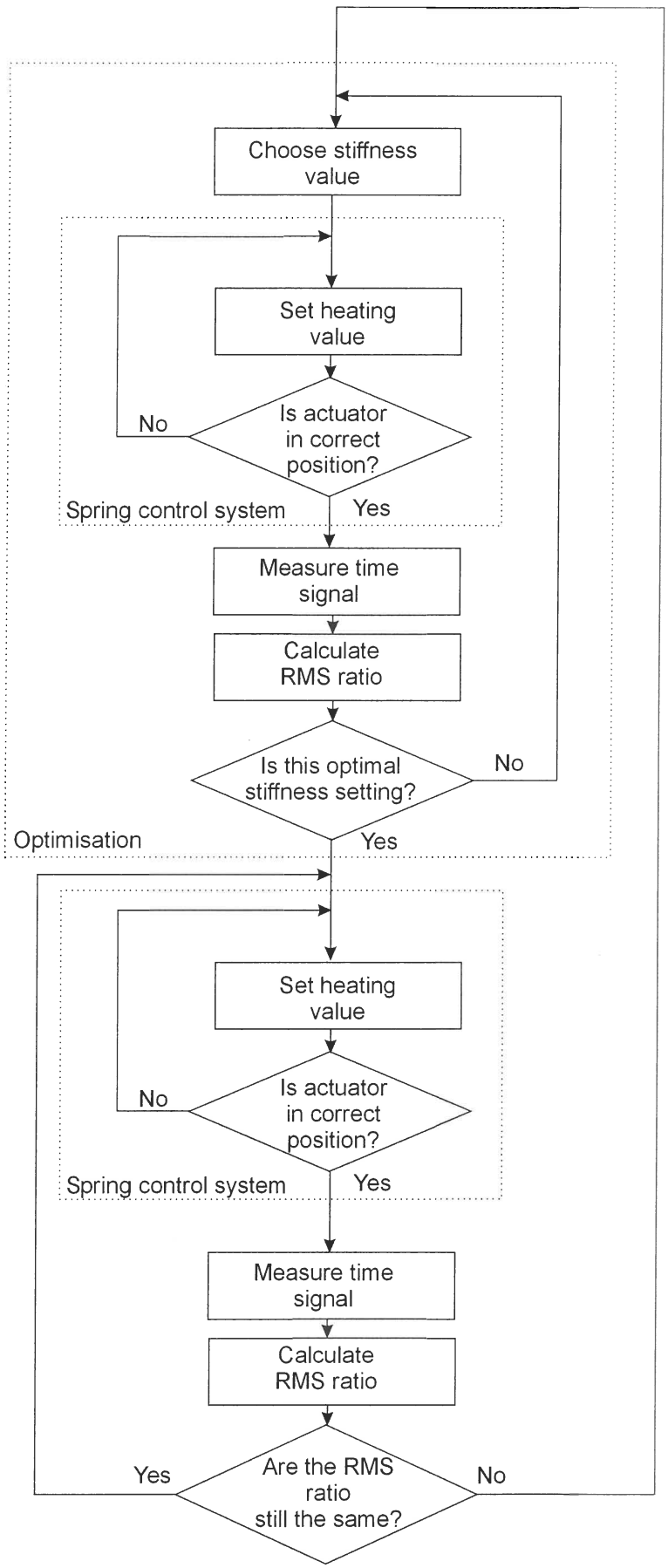

Figure 4. 25 Complete control system

well, it would make the optimisation a two variable optimisation. The whole structure of the control system would stay exactly the same.

4.6 Effect of variable damping

In section 4.4 the effect of the variable damping mechanism on the transmissibility graphs of the isolator was measured as given in Figure 4. 19. To illustrate how this change in damping can practically result in a lower RMS ratio, these graphs will be used to calculate the transmitted vibrations for various excitation conditions. The RMS ratio will be calculated and compared to each other to try and illustrate the gain that can be obtained by varying the damping.

The three graphs in Figure 4. 19 will be used for the calculations. To calculate the RMS ratio, the input and output time signals are needed. A theoretical signal will be created as input signal. This signal must represent tonal excitation together with wide band noise. The transmissibility of the isolator is in the frequency domain and therefore it is necessary to convert the input signal to the frequency domain by means of a FFT. Figure 4. 26 show the input signal that was used in the time and frequency domain. The excitation frequency was 23 Hz, the same frequency as the isolation frequency of the isolator.

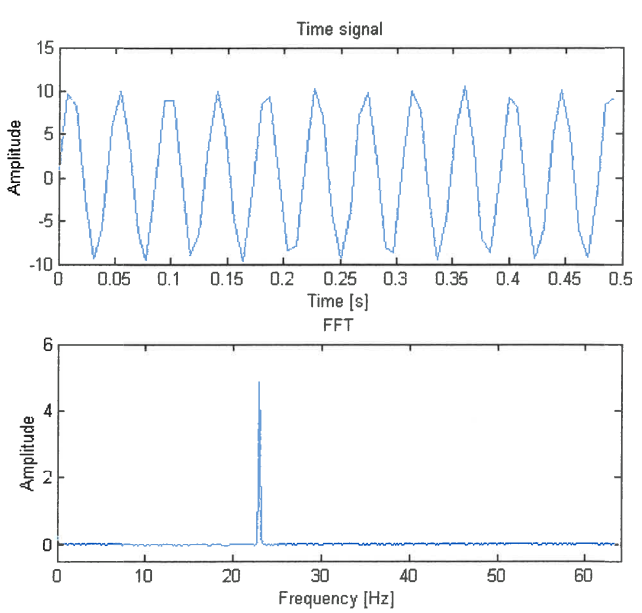

Figure 4. 26 Theoretical input signal with low noise levels

To determine the output FFT of the signal, the FFT in Figure 4. 26 must be multiplied by the transmissibility curves in Figure 4. 19. The result of this is given in Figure 4. 27.

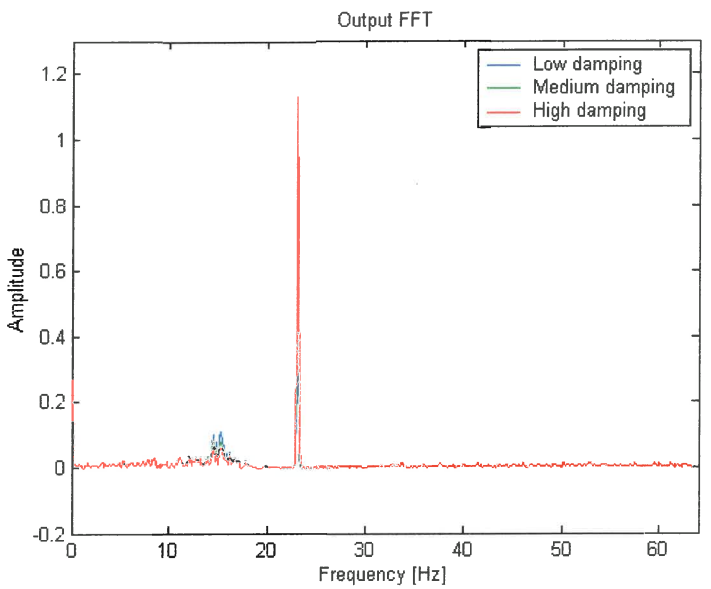

Figure 4. 27 Output FFT with low noise levels

To determine the RMS value of the output, the FFT of the output must be transformed back to the time domain by means of an IFFT. The RMS values of the input and output as well as the RMS ratio were calculated. This procedure was done three times for low, medium and high levels of noise and the results are as follows:

Table 4. 8 RMS ratio

Damping	**Low**	**Medium**	**High**
Low noise	0.076	0.103	0.146
Medium noise	0.201	0.195	0.204
High noise	0.364	0.317	0.278

From the results it is clear that higher damping results in a lower RMS ratio at higher noise levels. It is therefore shown that it is indeed necessary to change the damping to

be able to minimise the transmitted vibration in practical applications where noise is present. The graphs of the medium and high noise levels are presented in Appendix D.

4.7 Conclusion

In this chapter the design of the variable stiffness and damping isolator was addressed. The variable damping mechanism was first designed together with a stepper motor and driver to control the damping. The design of the whole isolator was done, drawings generated for manufacturing and all the parts manufactured. After assembling the isolator, the testing started. First the isolator was tested without water to be able to get accurate values for the stiffness and damping of the spring. After the addition of water the transmissibility of the isolator was measured and theoretical graphs fitted to it. A 58.77% variation in isolation frequency was achieved by shifting the isolation frequency from 22.8 Hz to 36.2 Hz. The viscous damping ratio was also changed from 0.0001 to 0.033. The second last section addressed the design and implementation of a control system to automatically tune the isolator to different excitation conditions. The final result was a tunable vibration isolator that can automatically adapt to changes in excitation conditions. The effect of the variable damping on the RMS ratio was investigated and it was found that the higher damping value did result in a lower RMS ratio value in noisy conditions as was expected.

CHAPTER 5

Conclusion

Vibrating machines are part of modern industry and in some cases the vibratory motion is an integral part of their working mechanism. These machines are therefore not suited to the implementation of a vibration absorber to minimise the vibration of the machine. In such cases it is necessary to make use of vibration isolator that minimise the vibration transmitted from the machine to surrounding bodies without effecting the vibratory motion of the machine. This study was done to develop a tunable vibration isolator that is able to automatically adapt itself to excitation conditions so that it can perform optimally all of the time. The isolator was based on the LIVE concept and it was decided to change the stiffness of the isolator to shift the isolation frequency. A variable damping mechanism was also designed and implemented to be able to control noise.

A variable stiffness spring was developed for implementation on the LIVE isolator. After investigation of different concepts, a compound leaf spring was chosen as a suitable concept for the spring. Circular springs were designed and manufactured to form the leafs of the spring. A wax actuator was used to separate the springs in the middle to obtain the stiffness change. The wax actuator was controlled by a closed loop displacement and velocity feedback system to form a smart actuator that could be controlled by a computer. The variable stiffness spring that was developed was capable of a change in stiffness of 2.7 times which is sufficient for implementation in a LIVE isolator. The spring was practical and the circular design made it suitable for the LIVE isolator.

The LIVE isolator was designed by using the derived equation for the transmissibility and isolation frequency. Equations for the damped natural and isolation frequency were also derived. A variable damping mechanism was implemented that consisted of a plate that was mounted in the tuning port of the isolator. Changing the angle of the plate caused a change in the damping of the isolator. The isolator was characterised in the laboratory on a servo-hydraulic actuator to determine the effect of the stiffness and damping change. The transmissibility functions were measured for all the different stiffness and damping settings. The variable stiffness resulted in a 58% shift in the isolation frequency from 22.8 Hz to 36.2 Hz. An isolation of 10% and lower was achieved over the whole stiffness range. The variable damping mechanism changed the viscous damping ratio from 0.001 to 0.033. The

effectiveness of the higher damping on the RMS ratio in noisy conditions was also illustrated.

A control system was developed to change the parameters of the isolator automatically and to tune the isolator optimally to various excitation conditions. The control system changed only the stiffness, but illustrated that it is possible to optimise the RMS ratio of the isolator by changing the parameters while in operation. The control system found the optimum settings and kept the isolator at that settings until the excitation conditions changed.

It is therefore concluded that a successful tunable vibration isolator was built which is able to automatically change its stiffness to adapt to excitation conditions. The isolator was able to isolate quite a wide range of frequencies, although not simultaneously. The objectives of this project were met, with exception that the damping was not automatically changed.

Future work that may be conducted would include a in depth study of the wax actuator to try and incorporate the heating and cooling elements inside the actuator, making it a very compact actuator. Response time of the actuator can be improved by using more effective ways of heating and especially cooling. Other work would be to find other more effective ways of separating the compound leaf spring to achieve better results. The control system can be developed further to include the damping control. Other applications for the variable stiffness spring could also be investigated. The design of the LIVE isolator with rolling diaphragms showed that it worked well and that opens the field to use any type of spring externally on such an isolator that could improve its performance.